Ancient DNA and lipid biomarkers quantify the climate sensitivity of highland shrubification in Iceland

David J. Harning [1, 2, *], Samuel Sacco [3], Jonathan H. Raberg [1, 4], Nicolò Ardenghi [1], Thor Thordarson [5], Julio Sepúlveda [1, 6], Gifford H. Miller [1], Áslaug Geirsdóttir [5]

[1] Institute of Arctic and Alpine Research, University of Colorado Boulder, Boulder, CO, USA
[2] Cooperative Institute for Research in Environmental Sciences, University of Colorado Boulder, Boulder, CO, USA
[3] Department of Ecology and Evolutionary Biology, University of California, Santa Cruz, USA
[4] Department of Geology and Geophysics, University of Wyoming, Laramie, WY, USA
[5] Faculty of Earth Sciences, University of Iceland, Reykjavík, Iceland
[6] Department of Geological Sciences, University of Colorado Boulder, Boulder, CO, USA

[*] Corresponding author: david.harning@colorado.edu

This is a non-peer-reviewed preprint.

Abstract

Future changes in high latitude shrubification are expected to lead to changes in ecosystem structure and positive climate feedbacks, but the rates and elevational range of shrubification are still poorly constrained. Using a sediment record from a small lake in Iceland's eastern highlands (422 m asl), we merge a sedimentary ancient DNA (*sed*aDNA) record of *Betula* with mean summer lake temperature (MST) reconstructed from bacterial branched glycerol dialkyl glycerol tetraethers (GDGTs) to quantify the extent and climate sensitivity of Icelandic woodlands. Our data show that during the Early Holocene MSTs were 2.75 ºC warmer than present and *Betula* woodlands were present in the lake‘s catchment, significantly higher than their current regional limit (250 to 350 m asl). During the Middle and Late Holocene, reconstructed MSTs are unreliable likely due to reducing conditions in the lake‘s water column inferred from archaeal isoprenoid GDGTs. However, relative temperature changes inferred from biogenic silica abundance indicate that the disappearance of *Betula* from the catchment was coeval with Little Ice Age cooling. Using Early Holocene warmth as a partial analog for future climate change, Coupled Model Intercomparison Project Phase 6 (CMIP6) ensemble projections suggest that the natural re-expansion of *Betula* woodlands to the eastern highlands is possible by 2100 CE, which would occupy >42 % of Iceland‘s land surface area.

1. Introduction

The range expansion of deciduous shrubs (i.e., shrubification) is a key feature of high-latitude ecological change (Tape et al., 2006; Myers-Smith et al., 2011; Elmendorf et al., 2012; Sweet et al., 2015). Not only does shrubification alter the structure of regional ecosystems (Elmendorf et al., 2012; Fauchald et al., 2017; Collins et al., 2018; Criado et al., 2025), it also has important implications for the global climate system. The expansion and increased height and density of woody shrubs reduces the surface albedo (Sturm et al., 2005) and increases atmospheric water vapor through evapotranspiration (Pearson et al., 2013). Both mechanisms amplify warming and are important feedback mechanisms for global paleoclimate (Thompson et al., 2022) and ice sheet models (Sommers et al., 2021). However, empirical reconstructions of past shrubification are needed for optimal model parametrization before they can be run forward under various emission scenarios. Recently, with the advent of advanced analytical techniques such as sedimentary ancient DNA (*sed*aDNA), robust empirical patterns of shrubification are emerging from northern high latitude lake sediment records that can support climate simulations (e.g., Crump et al., 2019, 2021; Alsos et al., 2021; Harning et al., 2023).

Shrubification reconstructions from islands during deglacial times, such as on Iceland, are particularly valuable as they constrain possible dispersal mechanisms for plant colonization as well as subsequent range expansion (Alsos et al., 2021; Harning et al., 2023). *Landnámabók*, the oldest source on the settlement of Iceland (c. 870 CE, 1080 cal yr BP) written in the first half of the 12th Century, claims that forests covered the shore to mountainsides when humans arrived ("*Í þann tíð vas Ísland viði vaxit á miðli fjalls ok fjoru*", Vésteinsson, 1998), which has been interpreted as widespread *Betula* (birch) woodlands at the time (~25 % land surface area, Smith, 1995). At lower elevation coastal sites, lake sediment records based on pollen and *sed*aDNA constrain postglacial *Betula* colonization patterns (e.g., Hallsdóttir, 1995; Alsos et al., 2021; Geirsdóttir et al., 2022; Harning et al., 2023, 2025). At higher elevations in Iceland, however, Holocene *Betula* records are limited to a single pollen record (Barðalækjartjörn, 413 m asl,) and two macrofossil records (Barðalækjartjörn and Vesturárdalur, 450 m asl, Wastl et al., 2001; Eddudóttir et al., 2016) (Fig. 1A). Unfortunately, due to long-distant transport, pollen is often an unreliable proxy for determining the first appearance of taxa on the landscape, while macrofossils are inconsistently preserved in the sedimentary record (Hyvärinen, 1970; Birks, 2003; Harning et al., 2023). Given the superior reliability of lake *sed*aDNA for reconstructing catchment-scale vegetation (Sjögren et al., 2017; Alsos et al., 2018; Capo et al., 2021), new Holocene *sed*aDNA records are needed from the Icelandic highlands.

Considering this knowledge gap, we first provide a high-resolution Holocene plant *sed*aDNA record from the lake Heiðarvatn (elevation 422 m asl), in the eastern highlands of Iceland (Fig. 1A). Second, we pair Heiðarvatn's *sed*aDNA record with mean summer lake temperature reconstructed from bacterial branched glycerol dialkyl glycerol tetraethers (brGDGTs) to quantify local Early Holocene summer warmth. Third, by focusing on the thermophilic woody taxon *Betula,* we compare Heiðarvatn's record with low- (52 to 151 m asl) to high-elevation (413 to 450 m asl) plant *sed*aDNA and macrofossil records to track Early Holocene shrubification in Iceland. Our paired *Betula* and summer temperature history allows us to place Early Holocene woodland conditions within the context of future warming scenarios and suggest that *Betula*, barring human intervention, is likely to naturally expand across the Icelandic highlands by the end of the 21st Century. In addition to insight on the Holocene evolution of Icelandic ecosystems and climate, our data provide targets for climate models incorporating positive woody vegetation feedbacks.

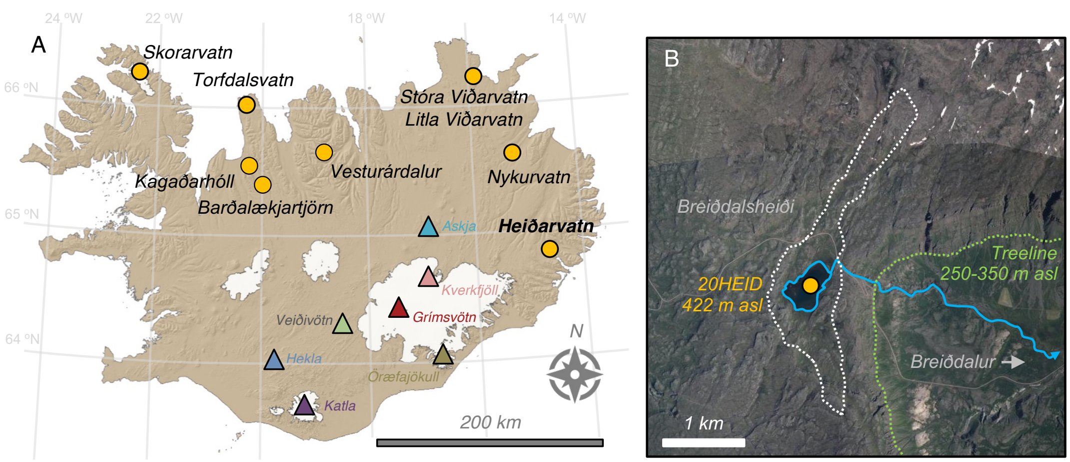

Fig. 1: Overview map of Iceland. (A) Location of Heiðarvatn in east Iceland related to other terrestrial (yellow) paleoclimate and vegetation records mentioned in the text. Active central volcanos (triangles) that produced tephra layers used in the age model are also marked. (B) Close-up of Heiðarvatn, its catchment (dotted white line), outflow (blue line), location of the 20HEID sediment core site (yellow), and modern *Betula* treeline in Breiðdalur (dotted green line). 2017 base image courtesy of Loftmyndir ehf.

2. Methods and Materials

2.1. Study area

Heiðarvatn (64.90 °N, 14.59 °W) is a relatively small lake with a surface area of 0.16 km^2 and max water depth of 15.1 m. The lake sits in Iceland's eastern highlands of Breiðdalsheiði (422 m asl, Fig. 1A) atop Tertiary volcanic bedrock (Harðarson et al., 2008) and drains to the east through one outflow into Breiðdalur (Fig. 1B). Soils within Heiðarvatn's catchment consist of brown to gleyic histosols and vitrosols (Arnalds and Gretarsson, 2001) and, based on our field visits in September

2019 and 2020, catchment vegetation is dominately comprised of moss heath and grassland or sparesly vegetated habitat. Modern *Betula* treeline is below Heiðarvatn in Breiðdalur between elevations of ~250 to 350 m asl (Fig. 1B).

Between September 2019 and September 2020, iButtons loggers (Thermochron DS1925L, Maxim Integrated Products) measured *in situ* surface and bottom lake water temperatures at 6-hour intervals (Fig. S1A, Raberg et al., 2021b). We also measured dissolved oxygen, specific conductivity, and pH with a multiparameter probe (HydroLab HL4, OTT HydroMet) at ~0.5-m increments along a vertical profile at our sediment core site in September 2019 and February 2020 (Fig. S1B-D, Raberg et al., 2023). These modern physicochemical water properties are used to guide our interpretation of lipid biomarker and *sed*aDNA data.

2.2. Sediment core and chronology

In February 2020, we recovered a 7.68 m long core from Heiðarvatn (20HEID) using a Bolivia piston coring system. 20HEID was collected in three overlapping drives (20HEID-04, 20HEID-01, and 20HEID-02), where the final drive reached refusal at the bottom of the lake and the surface core preserved the sediment-water interface. Sediment sections were photographed and measured for magnetic susceptibility (MS) at the Continental Scientific Drilling Facility (University of Minnesota) and used to splice the three sections into a single composite sediment record. Sealed core sections were stored at 4 °C at the University of Colorado Boulder until sampling.

Heiðarvatn's chronology relies on 11 visible tephra layers of known age as no plant macrofossils were found for radiocarbon (^{14}C) analysis. Each tephra layer was sampled along the vertical axis, sieved to isolate glass fragments between 125 and 500 µm, and embedded in epoxy plugs. At the University of Iceland, individual glass shards were analyzed on a JEOL JXA-8230 electron microprobe using an acceleration voltage of 15kV, beam current of 10 nA, and a beam diameter of 10 µm. The international A99 (basalt) and Lipari (rhyolite) standards were used to monitor for instrumental drift and maintain consistency between measurements. Tephra origin was then assessed using major oxide compositions, following the systematic procedures outlined in Jennings et al. (2014) and Harning et al. (2018a). Briefly, based on SiO_2 wt % vs total alkali (Na_2O+K_2O) wt %, we determined whether the tephra volcanic source is mafic (tholeiitic or alkalic), intermediate, and/or rhyolitic. From here, we objectively discriminate the source volcanic system through a detailed series of bi-elemental plots produced from available compositional data on Icelandic tephra. Source eruption was then determined using the geochemical fingerprint and relevant stratigraphic information. See Supporting Data for complete major oxide compositions.

A coarse-grained unit of sediment was identified between 544 and 583 cm depths and suspected to have been deposited as a slump in the sedimentary record. To test this, we sampled bounding bulk sediment for ^{14}C dating. Humic acids were extracted following the procedures of Abbott and Stafford (1996), graphitized at the Laboratory for AMS Radiocarbon Preparation and Research (University of Colorado Boulder), then measured by AMS at the W.M. Keck Carbon Cycle AMS Laboratory (University of California Irvine). AMS ^{14}C ages were then calibrated using the IntCal20 calibration curve (Reimer et al., 2020), which are statistically indistinguishable from each other (9780 ± 100 and 9590 ± 60 cal yr BP, Fig. 2A and Table S2).

We generated a Bayesian age model using the 11 tephra layers in the R package rbacon using default settings and the 'slump' function to account for the instantaneous deposition of sediment between 583 and 544 cm depths (Blaauw and Christen, 2011; R Core Team, 2020). While the calibrated ^{14}C humic acid dates are stratigraphically too old likely due to old carbon on the landscape (Geirsdóttir et al., 2009a), the similarity in ages along with the minerogenic nature of the sediment (high MS, Fig. 2C) suggests that this unit was deposited instantaneously. Therefore, these two dates were omitted from the final age model (Fig. 2A).

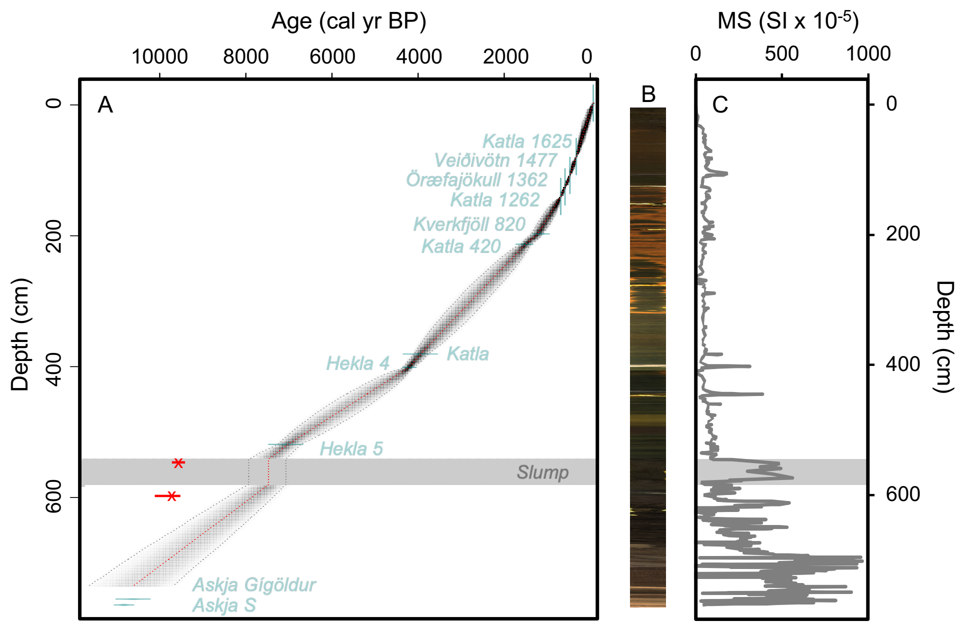

Fig. 2: Bayesian age model and lake sediment stratigraphy for Heiðarvatn. A) rbacon age model using tephra layers of known age (green), where solid red line reflects the median of model iterations, the outer gray lines denote the 95% confidence interval, and red data points reflect omitted sediment humic acid ^{14}C dates (n = 2), B) core image with exaggerated width for easier visibility, and C) magnetic susceptibility (MS, SI x 10^{-5}). Horizontal gray bar across panels A-C reflects the position of the instantaneous sediment slump that was removed from the age model. See Tables S1 and S2 for tephra layer and radiocarbon information, respectively.

2.3. Bulk sediment geochemistry

156 samples were taken and measured for total carbon (TC), total nitrogen (TN), and $\delta^{13}C$ (relative to VPDB) at the Stable Isotope Facility (University of California Davis). We did not decalcify samples due to the limited stock of inorganic carbon in and around the lake, and therefore take TC to reflect total organic carbon (TOC, see Ardenghi et al., 2024). Each sample was analyzed on a PDZ Europa ANCA-GSL elemental analyzer interfaced to a PDZ Europa 20-20 isotope ratio mass spectrometer. We also measured 181 samples for biogenic silica at the University of Colorado Boulder using a diffuse reflectance Fourier Transform Infrared Spectrometry (FTIRS) on a Bruker Vertex 70 with a Praying Mantis diffuse reflectivity accessory (Harrick). We report values in FTIRS - Fourier Transform Infrared Spectroscopy absorbance units (e.g., Harning et al., 2018b).

2.4. Lipid biomarkers

At the Organic Geochemistry Laboratory (University of Colorado Boulder), we freeze-dried 60 sediment samples (~1 to 10 g) and extracted each two times on a Dionex accelerated solvent extractor (ASE 350) using dichloromethane (DCM):methanol (9:1, v/v) at 100 ºC and 1500 psi. A 25 % aliquot of total lipid extracts (TLE) was taken for glycerol dialkyl glycerol tetraether (GDGT) analysis, resuspended in *n*-hexane:isopropanol (99:1, v/v), sonicated, vortexed, and then filtered using a 0.45 μm polytetrafluoroethylene (PTFE) syringe filter. Prior to analysis, samples were spiked with 10 ng of the C_{46} GDGT internal standard for GDGT quantification (Huguet et al., 2006). GDGTs were identified and quantified via high-performance liquid chromatography–mass spectrometry (HPLC-MS) following modified methods of Hopmans et al. (2016) on a Thermo Scientific Ultimate 3000 HPLC interfaced to a Q Exactive Focus Quadrupole-Orbitrap MS (Raberg et al., 2021a). Isoprenoid and branched GDGTs were identified based on their characteristic masses and elution patterns.

To reconstruct past environmental conditions, we explored a variety of published indices and temperature calibrations that rely on the distribution and fractional abundance of isoprenoid and branched GDGTs (isoGDGT and brGDGT, respectively). Briefly, we focused on the ratio of isoGDGT-0/crenarchaeol as a proxy for the relative abundance of archaeal methanogens (Blaga et al., 2009). For quantitative temperature estimates, we relied on an *in-situ* brGDGT calibration from Skorarvatn (Harning et al., 2020), a lake in NW Iceland (Fig. 1A), that capitalizes on the strong relationship between the unsaturation of alkenones (U^K_{37},), a separate class of lipids produced by haptophyte algae, and mean summer lake temperature (MST, D'Andrea et al., 2016):

$$U^K_{37} = -0.1540 \times [IIIa] + 0.3538 \times [Ia] + 1.0016 \times [IIIa'] - 0.7537$$

$$U^K_{37} = 0.0287 \times T \text{ (T S.E. = 1.3 °C)}$$

We assume that the reconstructed lake water temperatures reflect June, July, and August because these months reflect peak lake water temperatures in both lakes (Fig. S1A) when most alkenone synthesis should occur during haptophyte algal blooms (e.g., D'Andrea et al., 2016). We note that other brGDGT temperature calibrations exist for lake sediment, such as the MBT'_{5Me} and temperature for months above freezing (MAF) indices (Fig. S2, e.g., De Jonge et al., 2014; Raberg et al., 2021a; Otiniano et al., 2024). However, we opt for the MST calibration as the JJA months are most important for high-latitude plant communities (e.g., Elmendorf et al., 2012) and are common output of climate models (e.g., IPCC, 2021) needed for data-model comparisons.

2.5. sedaDNA metabarcoding

Our *sed*aDNA metabarcoding approach followed the same method used for two other recent Holocene lake sediment records from Iceland, Stóra and Litla Viðarvatn (Fig. 1A, Harning et al., 2023, 2025). Briefly, *sed*aDNA sampling (n = 59) was conducted immediately after splitting the sediment cores in a dedicated clean lab with no PCR products in the Trace Metal Lab (University of Colorado Boulder). *Sed*aDNA samples were collected from the same intervals as biomarker samples, as described above, ensuring that the two series are time locked. We performed sample extraction and processing in a dedicated ancient DNA laboratory (Paleogenomics Lab, University of California Santa Cruz). Based on a comparison of three sedimentary DNA extraction methods (Harning et al., 2025), we extracted lake sediment samples following Rohland et al. (2018). Complete methods for extraction, quantitative PCR (qPCR), *trnL* metabarcoding, sequencing, and bioinformatic processing are provided in the Supporting Information Text S1.

3. Results and Interpretation

3.1. Sediment core stratigraphy and chronology

The 7.68-m-long composite sediment core (20HEID) captures Heiðarvatn's entire Holocene sediment package as coring equipment reached refusal, which we interpret to reflect the basement bedrock, and the sediment-water interface was intact. Our Bayesian age model, which is based on 11 geochemically confirmed tephra layers with known ages (Table S1), has a relatively linear sedimentation rate from the Askja S tephra layer at the base of the record (10830 cal yr BP, Bronk

Ramsey et al., 2015) until the Hekla 4 tephra layer (4200 cal yr BP, Dugmore et al., 1995), where sedimentation rates increase before increasing again after the Kverkfjöll tephra layer (1130 cal yr BP) (Fig. 2A). Age model uncertainty is ~400 years during the Early Holocene and decreases towards present due to more frequent age control points (Fig. 2A). The base of the core at 768 cm (~10850 cal yr BP) up to 600 cm (~7800 cal yr BP) is comprised of dense laminated clay to silt and repeated, thick (cm to dm), coarse-grained tephra layers. Above 600 cm, the sediment transitions to organic gyttja (massive and laminated) with thinner (mm to cm), discrete tephra layers.

3.2. Geochemical paleoclimate proxies

Magnetic susceptibility (MS) shows relatively high values from the base of the record until ~7800 cal yr BP (Fig. 3A), reflecting a greater contribution of minerogenic material to the lake sediment possibly due to meltwater discharge from a retreating ice sheet as well as thick tephra layers. Periodic MS spikes after ~7800 cal yr BP are due to discrete tephra layers (Fig. 3A). Bulk organic geochemistry is characterized by %TOC ranging from 0.01 to 6.97 %, C/N ranging from 3.07 to 14.9, $\delta^{13}C$ ranging from -27.2 to -22.5 ‰, and BSi ranging from 11 to 61 FTIRs absorbance units (Fig. 3B-D). We do not include organic geochemistry analyses of the deglacial sediments older than ~7800 cal yr BP due to minimal organic matter content. Based on the composition of modern organic matter sources in Icelandic lakes (e.g., Geirsdóttir et al., 2020), bulk geochemistry of Heiðarvatn's sediment indicates relatively low contributions of aquatic sources compared to terrestrial plants and soil throughout the record (relatively high C/N and low $\delta^{13}C$, Fig. 3C-D). While generally stable, sediments between ~7800 and 7500 cal yr BP and younger than ~500 cal yr BP have higher proportions of aquatic sources (relatively low C/N and high $\delta^{13}C$, Fig. 3C-D). Finally, after the catchment stabilizes ~7800 cal yr BP, BSi indicates relatively high diatom productivity to ~4900 cal yr BP before generally decreasing towards present (Fig. 3E).

IsoGDGTs are present above the detection limit in all samples from Heiðarvatn. The ratio of isoGDGT-0/crenarchaeol ranges from 0.78 to 104, with values staying persistently elevated after ~5150 cal yr BP (Fig. 3F). Increased isoGDGT-0/crenarchaeol ratios likely indicate intervals of more reducing conditions (low dissolved oxygen concentrations) that promote archaeal methanogenesis (Blaga et al., 2009; Naeher et al., 2014). These reducing conditions could result from increased organic matter deposition and respiration in the lake sediment and/or low dissolved oxygen concentrations in the water column (Blaga et al., 2009; Naeher et al., 2014). As brGDGT concentrations have been shown to increase under anoxic water columns in other lakes (Weber et al., 2018; Baxter et al., 2024), the close correspondence between brGDGT concentrations and isoGDGT-0/crenarchaeol (Fig. S2B) suggests that the isoGDGT-0/crenarchaeol in Heiðarvatn reflects the redox state of the aquatic environment. Inferred increases in reduced conditions between ~6800 and 6220 cal yr BP and after 5150 cal yr BP are also supported by contemporaneous increases in %TOC (Fig. 3B, orange bars), where reduced oxygen exposure likely contributes to enhanced TOC preservation (Sobek et al., 2009). Given the modern development of Heiðarvatn's seasonal oxycline (bottom water anoxia, Fig. S1B), we assume that Holocene changes in reducing conditions were driven by winter water column stratification (e.g., Jane et al., 2023).

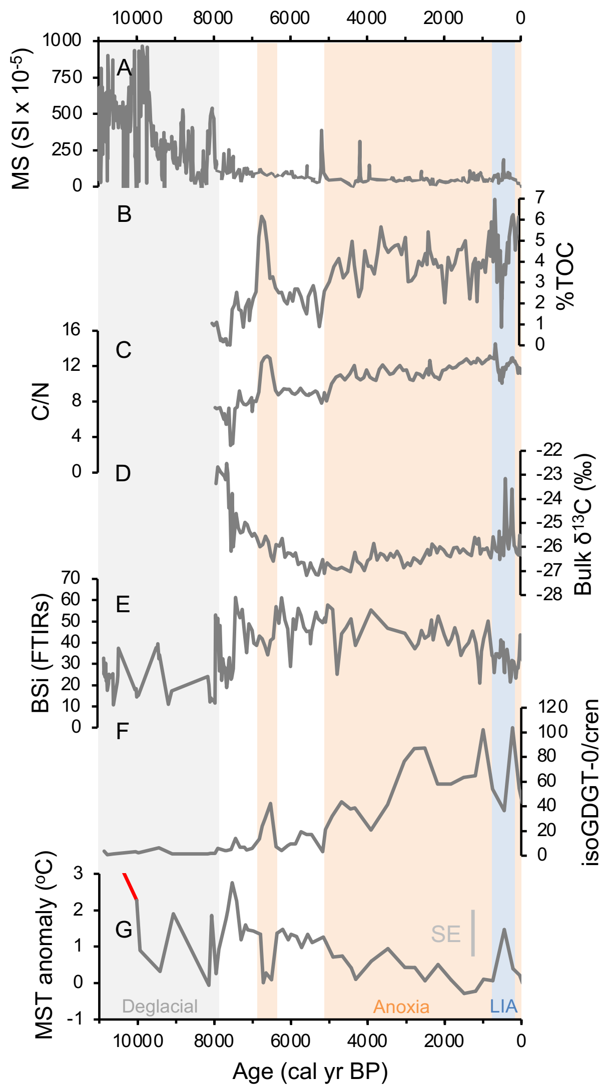

Fig. 3: Geochemical proxy records from Heiðarvatn. A) Magnetic susceptibility (MS, SI x 10^{-5}), B) % total organic carbon (TOC), C) elemental carbon/nitrogen, D) bulk $\delta^{13}C$ (‰), E) BSi (FTIRs absorbance units), F) isoGDGT-0/crenarchaeol, and G) brGDGT-inferred MST anomaly (ºC) and standard error (SE, gray), where red samples have $IR_{6Me} > 0.4$ (Fig. S2C). Gray bar reflects basal deglacial sediments. Orange bars reflect portions of the record potentially impacted by low oxygen conditions based on isoGDGT-0/crenarchaeol ratios. Blue bar highlights the Little Ice Age (LIA).

BrGDGTs are present above the detection limit in all samples from Heiðarvatn. The relative distribution of brGDGTs is similar to modern and Holocene Icelandic lake sediments (Harning et al., 2020, 2025; Raberg et al., 2021) and different from modern Icelandic soils (Raberg et al., 2024, Fig. S4A). This, along with relatively high ∑IIIa/∑IIa ratios (Fig. S4C, Xiao et al., 2016; Martin et al., 2019), suggests that brGDGTs are dominantly produced within the lake. Given the aquatic origin, we use a local Icelandic mean summer lake temperature (MST) brGDGT calibration developed from a lake in northwest Iceland, Skorarvatn (Fig. 3G, Harning et al., 2020). While this calibration was specifically developed for Skorarvatn (Fig. 1A), its application for

Heiðarvatn is reasonable given the lakes' similar water depths (25 vs 15.1 m depth, respectively), physicochemical water properties, and brGDGT distributions (Fig. S4A). Reconstructed MST anomalies (relative to modern, where modern = 0 ºC) show generally higher MST anomalies during the Early Holocene and lower during the Late Holocene. We note that for the three oldest samples, IR_{6Me} ratios close to and >0.4 (Fig. S2C) indicate that temperatures may be influenced by currently unknown non-thermal factors, and therefore, unreliable (Novak et al., 2025). Reducing conditions during the Middle and Late Holocene (~6800 and 6220 cal yr BP and < 5150 cal yr BP) may also alter lake microbial communities and result in relatively lower inferred temperatures (Weber et al., 2018; Zander et al., 2024; Raberg et al., 2025). While we cannot confirm a causal relationship, we note that step decreases in temperature occur in Heiðarvatn's record contemporaneous with isoGDGT/crenarchaeol increases (Fig. 3F-G), consistent with previously proposed changes in microbial community and associated temperature described elsewhere.

3.3. SedaDNA paleovegetation

Of 59 samples analyzed in Heiðarvatn, 55 yield amplifiable plant DNA using the *trnL* P6 loop primer set. The four samples that failed are located at the base of the sediment record in deglacial sediment and dated to >10,800 cal yr BP. Following data filtering, the *trnL* dataset yields 14,423,091 total assigned reads, with an average of 224,459 assigned reads per sample. The relative stability of qPCR cycle threshold (C_T) values, which reflect PCR efficiency and the quantity of suitable target sequences for amplification, reveal stable trends and indicate that the efficiency of PCR amplification of trnL targets is consistent throughout the record after ~10,800 cal yr BP (Fig. S3). Metabarcoding technical quality (MTQ) and analytical quality (MAQ) scores are below suggested low quality thresholds (0.75 and 0.1, respectively, Rijal et al., 2021) in some samples during the Early Holocene (Fig. S3). However, given that the quality scores correlate with species richness and species richness is always below 30 (Fig. S3), the low MTQ and MAQ scores are likely an artifact of the requirement that the 10 best represented barcode sequences are required for calculation (Rijal et al., 2021), and not necessarily an indication of poor DNA preservation. We identified 49 plant taxa across a range of plant functional groups throughout the sediment record. Species richness (calculated as total species identified per sample) generally increases throughout the Holocene in all plant functional groups apart from a small trough in species richness located between ~5000 and 3000 cal yr BP (Fig. 4). See Supporting Information Text S2 for further discussion of plant taxa.

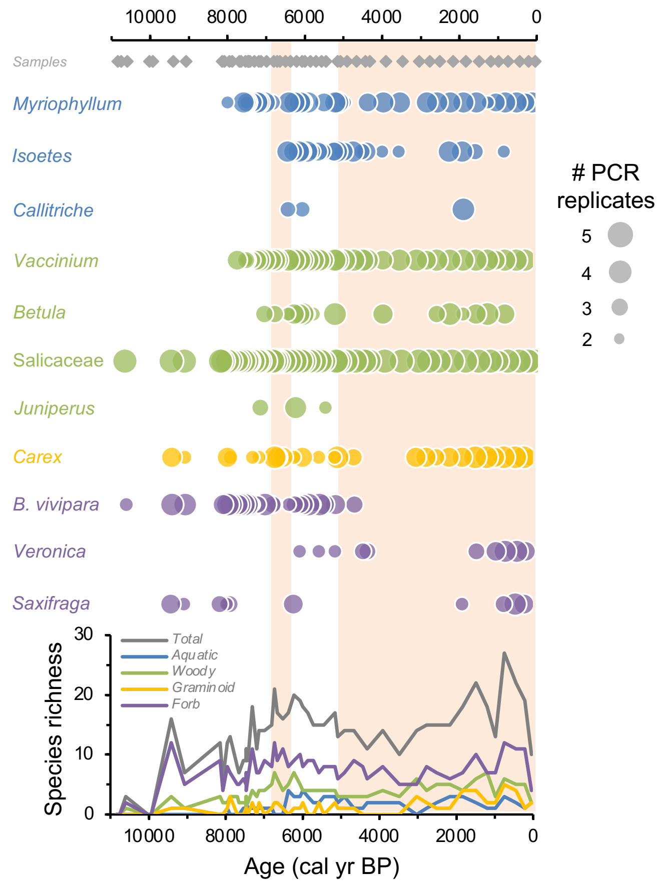

Fig. 4: Plant *sed*aDNA records from Heiðarvatn. Top: gray diamonds denote where samples were taken from and analyzed for DNA metabarcoding. Bubble plots reflect the presence/absence of select taxa, where the bubble size is proportional to the number of PCR replicates (1-5). Bottom: species richness shown for the total number of taxa as well as four plant functional groups (aquatic, woody, graminoid, and forb). Orange bars reflect portions of the record potentially impacted by low oxygen lake conditions based on isoGDGT-0/crenarchaeol ratios (Fig. 3F).

4. Discussion

Following the disintegration of the Icelandic Ice Sheet that covered the island during the Last Glacial Maximum (~28,000 to 22,000 cal yr BP, e.g., Patton et al., 2017), new territory was exposed for plants to colonize. Plant *sed*aDNA records from low-elevation lakes that deglaciated early document varied colonization efficiencies for different woody taxa. For instance, Salicaceae arrived in Torfdalsvatn and Stóra Viðarvatn's catchments (Fig. 1A, 52 and 151 m asl, respectively) up to 1700 years after deglaciation (Alsos et al., 2021; Harning et al., 2023). In contrast, *Betula* colonized later – ~2300 years after deglaciation of both lakes – potentially due to differences in environmental tolerances, species diversity within families, modes of reproduction, and seed morphology (Harning et al., 2023). *Betula*, which is found as either prostrate *B. Nana,* shrub-like *B. pubescens*, or hybrids thereof, is the main constituent of Icelandic woodlands (Hallsdóttir, 1995; Kristinsson, 2008; Thórsson et al., 2010), but cannot be separated to the species level using standard DNA metabarcoding approaches. Reconstructing the subsequent expansion of *Betula* woodlands to higher elevation, and what climate and environmental variables have shaped that history, has been limited by existing pollen and macrofossil records that are either impacted by long-distance transport or discontinous preservation in lake sediments as well as corresponding temperature histories (e.g., Hallsdóttir, 1995; Wastl et al., 2001; Eddudóttir et al., 2016; Geirsdóttir et al., 2022).

The Heiðarvatn (422 m asl) plant *sed*aDNA record provides important constraint on the timing of woody plant elevational expansion following deglaciation. As Iceland's residual ice caps and glaciers retreated into the highlands under a rapidly warming Early Holocene climate, the interior was largely ice free by ~10,000 cal yr BP (e.g., Geirsdóttir et al., 2009b; Larsen et al., 2012; Harning et al. 2016, 2020). This vast new territory allowed for *Betula* range expansion pending suitable climate and environmental conditions existed. Our data indicate that following deglaciation of Heiðarvatn's catchment by 10850 cal yr BP, *Betula* was established locally by 6990 cal yr BP (Fig. 5C). Another high-elevation plant *sed*aDNA record exists from the lake Nykurvatn (428 m asl), also in the eastern highlands (Fig. 1A), but the recovered sediment core does not include the interval prior to ~8600 cal yr BP through local deglaciation (Alsos et al., 2021). Despite this, Nykurvatn‘s record suggests that *Betula* was present earlier than in Heiðarvatn by at least ~8600 cal yr BP. Considering the two lake‘s proximity (85 km distance, Fig. 1A), this poses at least two explanatory possibilities: 1) taphonomic issues in the sediment record, such as oxic degradation (Harning et al., 2025), or 2) variable microclimates. Based on isoGDGT-0/cren, the Early Holocene portion of Heiðarvatn's record was likely oxic, but it is unlikely that this impacted DNA preservation as other taxa are present throughout this interval (Fig. 4), uniform C_T values do not indicate changes in *sed*aDNA preservation (Fig. S3), and other deep oxic lakes in Iceland have well-preserved DNA (Harning et al., 2025). Therefore, the different timing of *Betula*'s first appearance may relate to microclimate; in addition to temperature, precipitation is an important secondary control on *Betula* distribution (De Groot et al., 1997). Today, Heiðarvatn has a cooler and drier climate compared to Nykurvatn, partially due to prevailing southerly winds and the rain shadow north of Vatnajökull (e.g., Crochet et al., 2007; Crochet and Jóhannesson, 2011). While this pattern may have persisted throughout the Holocene as well, we currently lack independent temperature constraint from Nykurvatn and precipitation constraint from both lakes to test if a cooler and drier Early Holocene climate contributed to the relatively delayed establishment of local *Betula* around Heiðarvatn.

The highest elevation record of verified woodland presence are ^{14}C-dated *B. pubescens* macrofossils from the Vesturárdalur peat section (450 m asl, Wastl et al., 2001), north Iceland (Fig. 1A). Recalibrated ages using the latest IntCal20 ^{14}C curve (Reimer et al., 2020) indicate that *Betula* woodlands existed here from at least 7590 ± 100 to 6820 ± 150 cal yr BP (Fig. 5C). *B. pubescens* macrofossils from two nearby lake sediment records (Fig. 1A, Kagaðarhóll, 114 m asl, and Barðalækjartjörn, 413 m asl) indicate that *Betula* woodlands were present at slightly lower elevations in this area by >10,000 cal BP (Eddudóttir et al., 2015, 2016). These sites are important as, in contrast to the *sed*aDNA records which cannot distinguish *Betula* to the species level, macrofossils provide higher taxonomic resolution (i.e., *B. pubescens*). As Vesturárdalur indicates the presence of woodlands during the Early Holocene at elevations higher than Heiðarvatn and Nykurvatn, there is a higher probability that the *sed*aDNA *Betula* records from Heiðarvatn and Nykurvatn also reflect *B. pubescens*, or some hybridization with *B. nana*, at this time (e.g., Anamthawat-Jónsson et al., 2023). Collectively, the four high elevation sites of verified woody plant cover (Heiðarvatn, Nykurvatn, Barðalækjartjörn, and Vesturárdalur) are all above Iceland‘s modern *B. pubescens* treeline (Wöll, 2008). As ~42 % of Iceland‘s land surface area is below 400 m asl (National Land Survey of Iceland, 2020), this suggests that woodland covered at least 1.7x more land surface area than estimated when humans arrived (~25 %, Smith, 1995).

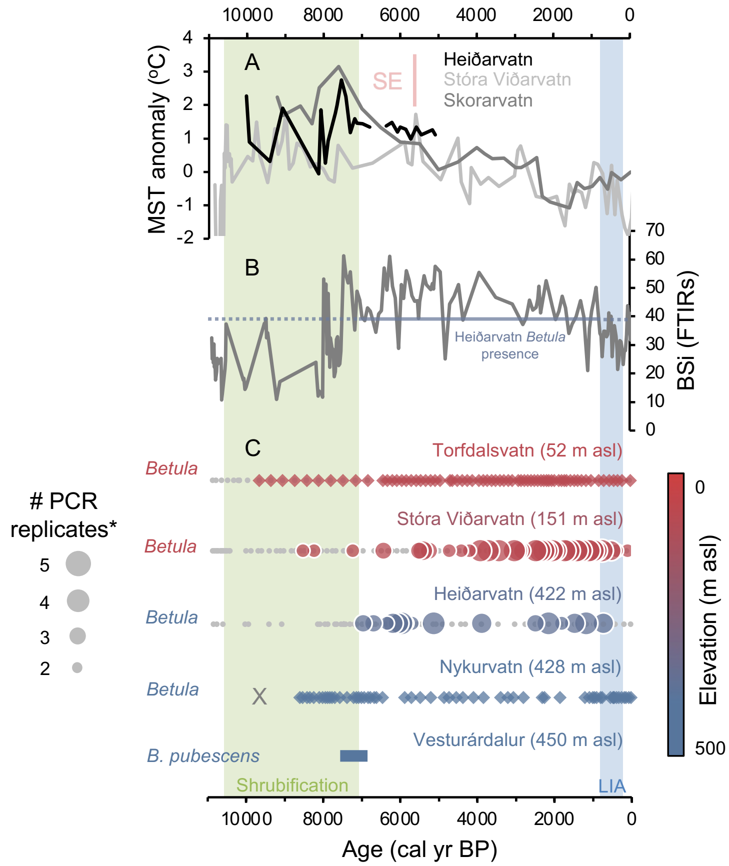

Fig. 5: Elevational range expansion of *Betula*. A) Heiðarvatn MST (and standard error, SE, red) anomaly excluding basal (IR_{6Me} > 0.4) and Late Holocene low oxygen sediment (ºC, black, this study) compared to Stóra Viðarvatn (gray, Harning et al., 2025a) and Skorarvatn (light gray, Harning et al., 2020). B) Heiðarvatn BSi (FTIRs absorbance units), where solid blue horizontal line reflects when *Betula* is present in the catchment. C) Icelandic woody plant records arranged from low to high elevation: Torfdalsvatn *sed*aDNA (Alsos et al., 2021), Stóra Viðarvatn *sed*aDNA (Harning et al., 2025a), Heiðarvatn *sed*aDNA (this study), Nykurvatn *sed*aDNA (Alsos et al., 2021), and Vesturárdalur macrofossils (*B. pubescens*, Wastl et al., 2001). All *sed*aDNA records show where all samples were analyzed (gray dots) where the X for Nykurvatn reflects its truncated base. For Stóra Viðarvatn and Heiðarvatn, *Betula* presence is indicated with a bubble whose size is proportional to the number of PCR replicates, whereas Torfdalsvatn and Nykurvatn are presence/absence and denoted with diamonds. Green bar highlights the expansion of woody plants from low to high elevation (i.e., shrubification) and blue bar highlights the Little Ice Age (LIA).

Heiðarvatn‘s brGDGT record during the Early Holocene indicates that MSTs were up to 2.75 ºC warmer than today at this site (Fig. 5A). A similar brGDGT MST anomaly is recorded in Skorarvatn, northwest Iceland, (+3.2 ºC, Fig. 5A, Harning et al., 2020), broadly supporting the temperature range observed in Heiðarvatn. In comparison, brGDGT MST anomalies from Stóra Viðarvatn, northeast Iceland, are relatively subdued during the Early Holocene (+1.75 ºC, Fig.

5A), but this difference is more likely due to the lake‘s substantially larger volume and greater energy required to warm lake water rather than differences in regional climate (Harning et al., 2025). Early Holocene MST anomalies from Heiðarvatn (+2.75 ºC) are within the range of all Coupled Model Intercomparison Project Phase 6 (CMIP6) ensemble projections for Iceland‘s 21st Century, including scenario SSP1-2.6, which reflects significant reductions in global CO_2 emissions (Fig. S5, Swark et al., 2019; IPCC, 2021). Despite different climate forcings for the two periods of warming (e.g., Fischer et al., 2018), the compatibility between MST reconstructions and CMIP6 simulations indicates that Heiðarvatn‘s Early Holocene climate may serve as a partial analogue of future climate. Given the strong sensitivity of modern *B. pubescens* treeline to MSTs in Iceland (Wöll, 2008) and projection of climate conditions suitable for their growth (Fig. S5), our data thus suggest that the natural expansion of woody shrubs from Breiðdalur to at least 422 m asl around Heiðarvatn is possible by 2100 CE.

Following peak Early Holocene warmth, Heiðarvatn‘s brGDGT MST record is currently unreliable due to potential impacts from reducing conditions. However, we presume that MSTs continued to decrease in line with quantitative temperature histories from Skorarvatn and Stóra Viðarvatn (Fig. 5A) and decreasing algal productivity as recorded in Heiðarvatn (BSi, Fig. 5B) as well as other Icelandic lake records (Geirsdóttir et al., 2020). Given the close connection between diatom productivity and warm season temperatures in Icelandic lakes (Geirsdóttir et al., 2009a), Heiðarvatn‘s BSi record provides a robust relative MST history for the last 11,000 years. Ultimately, decreasing Late Holocene relative MSTs is likely one reason why *Betula* disappeared from Heiðarvatn‘s catchment by 750 cal yr BP at the onset of the Little Ice Age (LIA, ~1250 CE, Fig. 5, Larsen et al., 2011; Geirsdóttir et al., 2013). The Little Ice Age at Heiðarvatn is further characterized by a temporary reduction in %TOC and C/N and increase in $\delta^{13}C$ (Fig. 3B-D), which may reflect a perennial frozen catchment that prohibited the mobilization of terrestrial organic matter into the lake as well as reduced aquatic productivity. Collectively, these geochemical lines of evidence point to natural reductions in relative summer temperature at 750 cal yr BP. If we take BSi absorbance values of ~38 as the „temperature“ threshold at which *Betula* disappeared from around the lake, similar values are found when *Betula* appeared at 6990 cal yr BP, which were generally maintained at or above this value until *Betula* disappeared at 750 cal yr BP (blue line , Fig. 5B). Hence, we argue that MST has been the dominant control that sustained the presence of *Betula* at Heiðarvatn between 6990 and 750 cal yr BP.

In addition to climate, pressure from early settlers and their livestock is also often cited as contributing to woodland degradation (e.g., Smith, 1995; Lawson et al., 2007; Alsos et al., 2021). However, the detection of early human presence in Icelandic sedimentary records using diagnostic geochemical techniques (e.g., mammalian fecal sterols and *sed*aDNA) has been challenging (Ardenghi et al., 2024; Harning et al., 2025). This may be partially due to the construction of livestock enclosures in Iceland’s early settlement history that initially prohibited free range to higher elevations like Heiðarvatn (Einarsson, 2015) and/or low population sizes of humans and livestock (Ardenghi et al., 2024; Harning et al., 2025). Assuming settlers were present no earlier than 1080 cal yr BP (*Landnámabók*), the continuous *sed*aDNA records from Heiðarvatn and Nykurvatn indicate that *Betula* remained a feature of higher elevations through this time (Fig. 5C) and therefore was not likely impacted by early human settlers. As *B. pubescens* is not present at these sites today, the Latest Holocene *sed*aDNA records likely reflect *B. nana*. Similar to low-elevation sites Stóra and Litla Viðarvatn in northeastern Iceland (Harning et al., 2025), these records collectively suggest that climate has been a stronger control on vegetation communites than human pressure. As such, these records provide robust constraint on climate-vegetation relationships needed for Earth system models.

Conclusions

Paired records of plant *sed*aDNA and brGDGT temperatures, supported by bulk geochemistry, from a small lake in Iceland's eastern highlands (Heiðarvatn) provide new insight into climate-ecosystem relationships in the northern North Atlantic. We find that during the Early Holocene, when mean summer lake temperatures (MST) from Heiðarvatn were up to 2.75 ºC warmer than today, *Betula* woodlands occupied at least 422 m asl. Compared with other *sed*aDNA records from the region, we hypothesize that the local timing of peak woodland cover was influenced by variable microclimates that impacted local temperature and precipitation patterns. During the Middle and Late Holocene, brGDGT temperatures are likely unreliable due to reducing conditions (low bottom water oxygen concentrations) and changes in the microbial communities. However, qualitative recontructions of MST based on biogenic silica indicate that *Betula* disappeared from the eastern highlands at the onset of the Little Ice Age, rather than earlier due to human settlement. This indiciates that climate has been the dominant driving force behind woodland cover in Iceland's eastern highlands during the Holocene. Therefore, these data provide a robust climate-vegetation constraint for Earth system models. By placing our data in the context of future climate projections, we suggest that with any future warming scenario, *Betula* may naturally expand and reoccupy high elevation regions of Iceland (>42 % land surface area) by 2100 CE.

Data Availability Statement

These data are currently being reviewed by the Arctic Data Center and will be publicly available by the time of final publication.

Acknowledgements

This study has been supported by the National Science Foundation (ARCSS-1836981 and OPP 2131589). We kindly thank Sveinbjörn Steinþórsson and Þór Blöndahl for lake coring assistance, Thomas Marchitto for access to the Trace Metal Lab at the University of Colorado Boulder, and Diana Brum de Silveira, Brooke Holman and Isiah Castro for lab assistance.

Author Contributions

ÁG, GHM, and JS funded the project; GHM, ÁG, DJH, JHR, and NA cored the lake; JHR, DJH and ÁG collected modern lake water quality data; DJH and ÁG sampled lake sediment; TT constructed the tephrochronology; DJH analyzed bulk geochemistry and GDGT datasets; SS performed DNA extractions and sequencing and DJH performed bioinformatics; DJH wrote the manuscript with contributions from all co-authors.

Competed Interests

The authors declare no competing interests.

References

Abbott, M. B., & Stafford, T. W. Jr. (1996). Radiocarbon geochemistry of modern and ancient Arctic lake systems, Baffin Island, Canada. *Quaternary Research, 45*, 300-311.

Alsos, I. G., Lammers, Y., Kjellman, S. E., Merkel, M. K. F., Bender, E. M., Rouillard, A., et al. (2021). Ancient sedimentary DNA shows rapid post-glacial colonisation of Iceland followed by relatively stable vegetation until the Norse settlement (Landnám) AD 870. *Quaternary Science Reviews, 259*, 106903.

Alsos, I. G., Lammers, Y., Yoccoz, N. G., Jørgensen, T., Sjögren, P., Gielly, L., et al. (2018). Plant DNA metabarcoding of lake sediments: how does it represent the contemporary vegetation. *PLOS ONE, 13*, e0195403.

Anamthawat-Jónsson, K., Karlsdóttir, L., Thórsson, Æ. Th., & Karlsdóttir, M. (2023). Microscopical palynology: Birch woodland expansion and species hybridisation coincide with periods of climate warming during the Holocene epoch in Iceland. *J. Microscopy, 291,* 128-141.

Ardenghi, N., Harning, D. J., Raberg, J. H., Holman, B. R., Thordarson, T., Geirsdóttir, Á., et al. (2024). A Holocene history of climate, fire, landscape evolution, and human activity in Northeast Iceland. *Climate of the Past, 20*, 1087-1123.

Arnalds, O., & Grétarsson, E. (2001). Soil map of Iceland. 2nd ed. *Agricultural University of Iceland, Reykjavík*. www.lbhi.is/desert

Baxter, A. J., Peterse, F., Verschuren, D., Maitituerdi, A., Waldmann, N., Sinninghe Damsté, J. S. (2024). Disentangling influences of climate variability and lake-system evolution on climate proxies derived from isoprenoid and branched glycerol dialkyl glycerol tetraethers (GDGTs): the 250 kyr Lake Chala record. *Biogeosciences, 21*, 2877-2908.

Birks, H. H. (2003). The importance of plant macrofossils in the reconstruction of Lateglacial vegetation and climate: examples from Scotland, western Norway, and Minnesota, USA. *Quaternary Science Reviews, 22*, 453–473.

Blaauw, M., & Christen, J. A. (2011). Flexible paleoclimate age-depth models using an autoregressive gamma process. *Bayesian Anal., 6,* 457–474.

Blaga, C. I., Reichart, G.-J., Heiri, O., & Sinninghe Damsté, J. S. (2009). Tetraether membrane lipid distribution in water-column particulate matter and sediments: A study from 47 European lakes along a north-south transect. *Journal of Paleolimnology, 41*, 535–540.

Bronk Ramsey, C., Albert, P. G., Blockley, S. P. E., Hardiman, M., Housley, R. A., Lane, C. S., et al. (2015). Improved age estimates for key Late Quaternary European tephra horizons in the RESET lattice. *Quat. Sci. Rev., 118*, 18–32.

Capo, E., Giguet-Covex, C., Rouillard, A., Nota, K., Heintzman, P. D., Vuillemin, A., et al. (2021). Lake sedimentary DNA research on past terrestrial and aquatic biodiversity: overview and recommendations. *Quaternary, 4*, 6.

Collins, C. G., Stajich, J. E., Weber, S. E., Pombubpa, N., & Diez, J. M. (2018). Shrub range expansion alters diversity and distribution of soil fungal communities across an alpine elevation gradient. *Molecular Ecology, 27*, 2461–2476.

Criado, M. G., Myers-Smith, I. H., Bjorkman, A. D., Elmendorf, S. C., Normand, S., Aastrup, P., et al. (2025). Plant diversity dynamics over space and time in a warming Arctic. *Nature*, https://doi.org/10.1038/s41586-025-08946-8.

Crochet, P., & Jóhannesson, T. (2011). A data set of gridded daily temperature in Iceland, 1949-2010. *Jökull, 61*, 1-17.

Crochet, P., Jóhannesson, T., Jónsson, T., Sigurðsson, O., Björnsson, H., Pálsson, F., et al. (2007). Estimating the spatial distribution of precipitation in Iceland using a linear model of orographic precipitation. *Journal of Hydrometerology, 8*, 1285-1306.

Crump, S. E., Fréchette, B., Power, M., Cutler, S., de Wet, G., Raynolds, M. K., et al. (2021). Ancient plant DNA reveals High Arctic greening during the last interglacial. *Proceedings of the National Academy of Sciences, 118*, 1–9.

Crump, S. E., Miller, G. H., Power, M., Sepúlveda, J., Dildar, N., Coghlan, M., et al. (2019). Arctic shrub colonization lagged peak postglacial warmth: Molecular evidence in lake sediment from Arctic Canada. *Global Change Biology, 25*, 4244–4256.

D'Andrea, W. J., Theroux, S., Bradley, R. S., & Huang, X. (2016). Does phylogeny control U^{K}_{37}-temperature sensitivity? Implications for lacustrine alkenone paleothermometry. *Geochimica et Cosmochimica Acta, 175*, 168–180.

De Groot, W. J., Thomas, P. A., & Wein, R. W. (2007). *Betula nana* L. and *Betula glandulosa* Michx. *Journal of Ecology, 85*, 241-264.

De Jonge, C., Hopmans, E. C., Zell, C. I., Kim, J. H., Schouten, S., & Sinninghe Damsté, J. S. (2014). Occurrence and abundance of 6-methyl branched glycerol dialkyl glycerol tetraethers in soils: implications for palaeoclimate reconstruction. *Geochemica et Cosmochimica Acta, 141*, 97-112.

Dugmore, A. J., Cook, G. T., Shore, J. S., Newton, A. J., Edwards, K. J., & Larsen, G. (1995). Radiocarbon dating tephra layers in Britain and Iceland. *Radiocarbon, 37*, 379–388.

Eddudóttir, S. D., Erlendsson, E., & Gísladóttir, G. (2015). Life on the periphery is tough: vegetation in Northwest Iceland and its responses to early-Holocene warmth and later climate fluctuations. *The Holocene, 25*, 1437–1453.

Eddudóttir, S. D., Erlendsson, E., Tinganelli, L., & Gísladóttir, G. (2016). Climate change and human impact in a sensitive ecosystem: the Holocene environment of the northwest Icelandic highland margin. *Boreas, 45*, 715–728.

Einarsson, Á. (2015). Viking Age fences and early settlement dynamics in Iceland. *Journal of the North Atlantic, 27*, 1-21.

Elmendorf, S. C., Henry, G. H. R., Hollister, R. D., Björck, R. G., Boulanger-Lapointe, N., Cooper, E. J., et al. (2012). Plot-scale evidence of tundra vegetation change and links to recent summer warming. *Nature Climate Change, 2*, 453-457.

Fauchald, P., Park, T., Tømmervik, H., Myneni, R, & Hausner, V. H. (2017). Arctic greening from warming promotes declines in caribou populations. *Science Advances, 3*, e1601365.

Fischer, H., Meissner, K. J., Mix, A. C., Abram, N. J., Austermann, J., Brovkin, V., et al. (2018). Palaeoclimate constraints on the impact of 2 ºC anthropogenic warming and beyond. *Nature Geoscience, 11,* 474-485.

Geirsdóttir, Á., Harning, D. J., Miller, G. H., Andrews, J. T., Zhong, Y., & Caseldine, C. (2020). Holocene history of landscape instability in Iceland: Can we deconvolve the impacts of climate, volcanism and human activity? *Quaternary Science Reviews, 249*, 106633.

Geirsdóttir, Á., Miller, G. H., Andrews, J. T., Harning, D. J., Anderson, L. S., Larsen, D. J., et al. (2019). The onset of Neoglaciation in Iceland and the 4.2 ka event. *Climate of the Past, 15*, 25-40.

Geirsdóttir, Á., Miller, G. H., Axford, Y., & Ólafsdóttir, S. (2009b). Holocene and latest Pleistocene climate and glacier fluctuations in Iceland. *Quaternary Science Reviews, 28*, 2107-2118.

Geirsdóttir, Á., Miller, G. H., Larsen, D. J., & Ólafsdóttir, S. (2013). Abrupt Holocene climate transitions in the northern North Atlantic region recorded by synchronized lacustrine records in Iceland. *Quaternary Science Reviews, 70*, 48–62.

Geirsdóttir, Á., Miller, G. H., Thordarson, T., & Ólafsdóttir, S. (2009a). A 2000 year record of climate variations reconstructed from Haukadalsvatn, West Iceland. *Journal of Paleolimnology, 41*, 95-115.

Geirsdóttir, Á., Miller, G. H., Harning, D. J., Hannesdóttir, H., Thordarson, T., & Jónsdóttir, I. (2022). Recurrent outburst floods and explosive volcanism during the Younger Dryas-Early Holocene deglaciation in south Iceland: evidence from a lacustrine record. *Journal of Quaternary Science, 37*, 1006-1023.

Hallsdóttir, M. (1995). On the pre-settlement history of Icelandic vegetation. *Búvísindi, 9*, 17-29.

Harðarson, B. S., Fitton, J. G., & Hjartarson, Á. (2008). Tertiary volcanism in Iceland. *Jökull, 58*, 161–178.

Harning, D. J., Curtin, L., Geirsdóttir, Á., D'Andrea, W. J., Miller, G. H., & Sepúlveda, J. (2020). Lipid biomarkers quantify Holocene summer temperature and ice cap sensitivity in Icelandic lakes. *Geophysical Research Letters, 47*, 1–11.

Harning, D. J., Geirsdóttir, Á., & Miller, G. H. (2018b). Punctuated Holocene climate of Vestfirðir, Iceland, linked to internal/external variables and oceanographic conditions. *Quaternary Science Reviews, 189*, 31–42.

Harning, D. J., Geirsdóttir, Á., Miller, G. H., & Zalzal, K. (2016). Early Holocene deglaciation of Drangajökull, Vestfirðir, Iceland. *Quaternary Science Reviews, 153*, 192-198.

Harning, D. J., Sacco, S., Anamthawat-Jónsson, K., Ardenghi, N., Thordarson, T., Raberg, J. H., et al. (2023). Delayed postglacial colonization of *Betula* in Iceland and the circum North Atlantic. *eLife, 12*, RP87749.

Harning, D. J., Thordarson, T., Geirsdóttir, Á., Zalzal, K., & Miller, G. H. (2018a). Provenance, stratigraphy and chronology of Holocene tephra from Vestfirðir, Iceland. *Quaternary Geochronology, 46*, 59-76.

Harning, D. J., Sacco, S., Raberg, J. H., Ardenghi, N., Sepúlveda, J., Shapiro, B., et al. (2025). A dual lake approach reveals the impact of Holocene oxygen availability and climate on molecular proxy records in the sub-Arctic. *Nature Communications Earth & Environment*, in revision.

Hopmans, E. C., Schouten, S., & Sinninghe Damsté, J. S. (2016). The effect of improved chromatography on GDGT-based palaeoproxies. *Organic Geochemistry, 93*, 1–6.

Huguet, C., Hopmans, E. C., Febo-Ayala, W., Thompson, D. H., Sinninghe Damsté, J. S., & Schouten, S. (2006). An improved method to determine the absolute abundance of glycerol dibiphytanyl glycerol tetraether lipids. *Organic Geochemistry, 37*, 1036–1041.

Hyvärinen, H. (1970). Flandrian pollen diagrams from Svalbard. *Geografiska Annaler, 52*, 213–222.

IPCC (2021). Summary for Policymakers. In: Climate Change 2021: The Physical Science Basis. Contribution of Working Group I to the Sixth Assessment Report of the Intergovernmental Panel on Climate Change [Masson-Delmotte, V., P. Zhai, A. Pirani, S. L. Connors, C. Péan, S. Berger, N. Caud, Y. Chen, L. Goldfarb, M. I. Gomis, M. Huang, K. Leitzell, E. Lonnoy, J.B.R. Matthews, T. K. Maycock, T. Waterfield, O. Yelekçi, R. Yu and B. Zhou (eds.)]. Cambridge University Press.

Jane, S. F., Mincer, J. L., Lau, M. P., Lewis, A. S. L., Stetler, J. T., & Rose, K. C. (2023). Longer duration of seasonal stratification contributes to widespread increases in lake hypoxia and anoxia. *Global Change Biology, 29*, 1009-1023.

Jennings, A. E., Thordarson, T., Zalzal, K., Stoner, J., Hayward, C., Geirsdóttir, Á., et al. (2014). Holocene tephra from Iceland and Alaska in SE Greenland shelf sediments. In: Austin WEN, Abbott PM, Davies SM, Pearce NJG, Wastegård S. (Eds.). Marine Tephrochronology. Geological Society, London, Special Publications, p. 398.

Kristinsson, H. (2008). Íslenskt plöntutal, blómplöntur og byrkningar. *Fjölrit Náttúrufræðistofnunar, 51*, 1–58.

Larsen, D. J., Miller, G. H., Geirsdóttir, Á., & Thordarson, T. (2011). A 3000-year varved record of glacier activity and climate change from the proglacial lake Hvítárvatn. *Quaternary Science Reviews, 30,* 2715-2731.

Larsen, D. J., Miller, G. H., Geirsdóttir, Á., & Ólafsdóttir, S. (2012). Non-linear Holocene climate evolution in the North Atlantic: a high-resolution, multi-proxy record of glacier activity and environmental change from Hvítárvatn, central Iceland. *Quaternary Science Reviews, 39*, 14-25.

Lawson, I. T., Gathorne-Hardy, F. J., Church, M. J., Newton, A. J., Edwards, K. J., Dugmore, A. T., et al. (2007). Environmental impacts of the Norse settlement: palaeoenvironmental data from Mývatnssveit, northern Iceland. *Boreas, 36,* 1-19.

Martin, C., Ménot, G., Thouvenay, N., Davtian, N., Andrieu-Ponel, V., Reille, M., et al. (2019). Impact of human activities and vegetation changes on the tetraether sources in Lake St Front (Massif Central, France). *Organic Geochemistry, 135*, 38-52.

Myers-Smith, I. H., Forbes, B. C., Wilmking, M., Hallinger, M., Lantz, T., Blok, D., et al. (2011). Shrub expansion in tundra ecosystems: dynamics, impacts and research priorities. *Environmental Research Letters, 6*, 045509.

Naeher, S., Peterse, F., Smittenberg, R. H., Niemann, H., Zigah, P. K., & Schubert, C. J. (2014). Sources of glycerol dialkyl glycerol tetraethers (GDGTs) in catchment soils, water column and sediments of Lake Rotsee (Switzerland)—Implications for the application of GDGT-based proxies for lakes. *Organic Geochemistry, 66*, 164–173.

National Land Survey of Iceland, 2020. ÍslandsDEM version 1.0, https://gatt.lmi.is/geonetwork/srv/eng/catalog.search#/metadata/e6712430-a63c-4ae5-9158-c89d16da6361.

Novak, J. B., Russell, J. M., Lindemuth, E. R., Prokopenko, A. A., Pérez-Angel, L., Zhao, B., et al. (2025). The branched GDGT isomer ratio refines lacustrine paleotemperature estimates. *Geochemistry, Geophysics, Geosystems, 26*, e2024GC012069.

Otiniano, G. A., Porter, T. J., Phillips, M. A., Juutinen, S., Weckström, J. B., & Heikkilä, M. P. (2024). Reconstructing warm-season temperatures using brGDGTs and assessing biases in Holocene temperature records in northern Fennoscandia. *Quaternary Science Reviews, 329*, 105555.

Pearson, R. G., Phillips, S. J., Loranty, M. M., Beck, P. S. A., Damoulas, T., Knight, S.J., et al. (2013). Shifts in Arctic vegetation and associated feedbacks under climate change. *Nature Climate Change, 3*, 673–677.

Raberg, J. H., Crump, S. E., de Wet, G., Harning, D. J., Miller, G. H., Geirsdóttir, Á., et al. (2024). BrGDGT lipids in cold regions reflect summer soil temperature and seasonal soil water chemistry. *Geochimica et Cosmochimica Acta, 369*, 111-125.

Raberg, J. H., de Wet, G., Geirsdóttir, Á., Sepúlveda, J., & Miller, G.H. (2025). Oxygen depletion in lake waters may skew brGDGT-inferred temperatures by more than 10 ^{o}C. *Geophysical Research Letters,* accepted.

Raberg, J. H., Harning, D. J., Crump, S. E., De Wet, G., Blumm, A., Kopf, S., et al. (2021a). Revised fractional abundances and warm-season temperatures substantially improve brGDGT calibrations in lake sediments. *Biogeosciences, 18*, 3579–3603.

Raberg, J., Harning, D., Geirsdóttir, Á., Sepúlveda, J., & Miller, G. (2021b). Soil and lake water temperatures of Iceland (2019-2021). Arctic Data Center [data set], http://doi.org/10.18739/A2XP6V46R.

Raberg, J., Harning, D., Geirsdóttir, Á., Sepúlveda, J., & Miller, G. (2023). Water chemistry profiles of lakes in Iceland (2019-2021). Arctic Data Center [data set], http://doi.org/10.18739/A26688K7F.

R Core Team (2021). R: A language and environment for statistical computing. Vienna, Austria: R Foundation for Statistical Computing, https://www.R-project.org/.

Reimer, P. J., Austin, W. E. N., Bard, E., Bayliss, A., Blackwell, P. G., Bronk Ramsey, C., et al. (2020). The IntCal20 northern hemisphere radiocarbon age calibration curve (0-55 cal kBP). *Radiocarbon, 62*, 725-757.

Rijal, D. P., Heintzman, P. D., Lammers, Y., Yoccoz, N. G., Lorberau, K. E., Pitelkova, I., et al. (2021). Sedimentary ancient DNA shows terrestrial plant richness continuously increased over the Holocene in northern Fennoscandia. *Science Advances, 7*, 1-16.

Rohland, N., Glocke, I., Aximu-Petri, A., & Meyer, M. (2018). Extraction of highly degraded DNA from ancient bones, teeth and sediments for high-throughout sequencing. *Nature Protocols, 13,* 2447-2461.

Sjögren, P., Edwards, M. E., Gielly, L., Langdon, C. T., Croudace, I. W., Merkel, M. K. F., et al. (2017). Lake sedimentary DNA accurately records 20th Century introductions of exotic conifers in Scotland. *New Phytologist, 213*, 929–941.

Smith, K. P. (1995). Landnám: the settlement of Iceland in archaeological and historical perspective. *World Archaeol., 26*, 319-347.

Sobek, S., Durisch-Kaiser, E., Zurbrügg, R., Wongfun, N., Wessels, M., Pasche, N., et al. (2009). Organic carbon burial efficiency in lake sediments controlled by oxygen exposure time and sediment source. *Limnology and Oceanography, 54*, 2243-2254.

Sommers, A. N., Otto-Bliesner, B. L., Lipscomb, W. H., Lofverstrom, M., Shafer, S. L., Bartlein, P. J., et al. (2021). Retreat and regrowth of the Greenland Ice Sheet during the Last Interglacial as simulated by the CESM2-CISM2 coupled climate-ice sheet model. *Paleoceanography and Paleoclimatology, 36*, e2021PA004272.

Sturm, M., Douglas, T., Racine, C., & Liston, G. E. (2005). Changing snow and shrub conditions affect albedo with global implications. *Journal of Geophysical Research, 110*, 1–13.

Swart, N. C., Cole, J. N. S., Kharin, V. V., Lazare, M., Scinocca, J. F., Gillett, N. P., et al. (2019). CCCma CanESM5 model output prepared for CMIP6 ScenarioMIP. *Earth System Grid Federation*. https://doi.org/10.22033/ESGF/CMIP6.1317.

Sweet, S. K., Griffin, K. L., Steltzer, H., Gough, L., & Boelman, N. T. (2015). Greater deciduous shrub abundance extends tundra peak season and increases modeled net CO_2 uptake. *Global Change Biology, 21*, 2394-2409.

Tape, K., Sturm, M., & Racine, C. (2006). The evidence for shrub expansion in Northern Alaska and the Pan-Arctic. *Global Change Biology, 12*, 686–702.

Thompson, A. J., Zhu, J., Poulsen, C. J., Tierney, J. E., & Skinner, C. B (2022). Northern Hemisphere vegetation change drives a Holocene thermal maximum. *Science Advances, 8*, eabj6535.

Thórsson, Æ. Th., Pálsson, S., Lascoux, M., Anamthawat-Jónsson, K. (2010). Introgression and phylogeography of *Betula nana* (diploid), *B. pubescens* (triploid) and their triploid hybrids in Iceland inferred from cpDNA haplotype variation. *J. Biogeogr., 37,* 2098-2110.

Vésteinsson, O. (1999). "Patterns of Settlement in Iceland: A Study in Prehistory." *Saga-Book*, vol. 25, pp. 1–29.

Wastl, M., Stötter, J., & Caseldine, C. (2001). Reconstruction of Holocene variations of the upper limit of tree or shrub birch growth in Northern Iceland based on evidence from Vesturárdalur-Skíðadalur, Tröllaskagi. *Arctic, Antarctic, and Alpine Research, 33*, 191-203.

Weber, Y., Sinninghe Damste, J. S., Zopfi, J., De Jonge, C., Gilli, A., Schubert, C. J., et al. (2018). Redox-dependent niche differentiation provides evidence for multiple bacterial sources of glycerol tetraether lipids in lakes. *Proceedings of the National Academy of Sciences, 115*, 10926–10931.

Wöll, C. (2008). Treeline of mountain birch (*Betula pubescens* Ehrh.) in Iceland and its relationship to temperature. MSc Thesis, Technische Universität Dresden.

Xiao, W., Wang, Y., Zhou, S., Hu, L., Yang, H., & Xu, Y. (2016). Ubiquitous production of branched glycerol dialkyl glycerol tetraethers (brGDGTs) in global marine environments: a new source indicator for brGDGTs. *Biogeosciences, 13*, 5883-5894.

Zander, P. D., Böhl, D., Sirocko, F., Auderset, A., Haug, G. H., & Martínez-García, A. (2024). Reconstruction of warm-season temperatures in central Europe during the past 60000 years from lacustrine branched glycerol dialkyl glycerol tetraethers (brGDGTs). *Climate of the Past, 20,* 841-864.